

First-order transition features of the triangular Ising model with nearest- and next-nearest-neighbor antiferromagnetic interactions

A. Malakis^{*}, N. G. Fytas and P. Kalozoumis

*Department of Physics, Section of Solid State Physics, University of Athens,
Panepistimiopolis, GR 15784 Zografos, Athens, Greece*

Abstract

We implement a new and accurate numerical entropic scheme to investigate the first-order transition features of the triangular Ising model with nearest-neighbor (J_{nn}) and next-nearest-neighbor (J_{nnn}) antiferromagnetic interactions in ratio $R = J_{nn}/J_{nnn} = 1$. Important aspects of the existing theories of first-order transitions are briefly reviewed, tested on this model, and compared with previous work on the Potts model. Using lattices with linear sizes $L = 30, 40, \dots, 100, 120, 140, 160, 200, 240, 360$ and 480 we estimate the thermal characteristics of the present weak first-order transition. Our results improve the original estimates of Rastelli et al. and verify all the generally accepted predictions of the finite-size scaling theory of first-order transitions, including transition point shifts, thermal, and magnetic anomalies. However, two of our findings are not compatible with current phenomenological expectations. The behavior of transition points, derived from the number-of-phases parameter, is not in accordance with the theoretically conjectured exponentially small shift behavior and the well-known double Gaussian approximation does not correctly describe higher correction terms of the energy cumulants. It is argued that this discrepancy has its origin in the commonly neglected contributions from domain wall corrections.

Key words: first-order transitions, triangular Ising model-
superantiferromagnetism, entropic sampling
PACS: 05.50+q, 75.10.Hk, 05.10.Ln, 64.60.Fr

^{*} Corresponding author.

Email address: amalakis@phys.uoa.gr (A. Malakis).

1 Introduction

Generalizations of the Ising model including further than nearest-neighbor interactions may give rise to complicated spatial orderings and produce complex and rich critical behavior [1,2]. The transitions between ordered and disordered phases may be continuous or of first-order with a tricritical point between them. The exactly soluble Ising model in $d = 2$ [3] with the addition of next-nearest-neighbor interactions becomes an analytically intractable problem and an understanding of the effects of adding such further couplings on the critical behavior of the system is an open important problem of great theoretical and experimental interest. We will be particularly interested in cases involving competing interactions with ground-state arrangements that mimic a sublattice order or superantiferromagnetic (SAF) order in which ferromagnetic lines along the directions of the lattice alternate with lines of opposite oriented spins. Such models are of great theoretical and experimental interest. They simulate various types of antiferromagnets [4,5,6,7,8], but also important models of alloy orderings [4]. Due to the well-known correspondence between spin systems and lattice gas, they provide an understanding of the behavior of adsorbed gases on crystal surfaces [9,10]. It should be noted here that, remarkable efforts have been made to predict the order of the transition according to the Landau-Lifshitz rules, which, on the basis of group theory arguments, select the ordered configurations that can be reached from the disordered phase by a continuous transition [4,11]. K. Binder [4] has reviewed these rules and has also pointed out well-known counter-examples, emphasizing the experimental difficulties in distinguishing a weak first-order transition from a second-order transition.

Second-order transitions are more special than first-order transitions, but they are theoretically much better understood. At a first-order transition there is no diverging correlation length, and in general one cannot restrict attention to long wavelength phenomena, thus no universality, as in critical phenomena, is to be expected. Furthermore, it is well known that antiferromagnetic arrangements, with several order-parameter components, may be produced by the competition of the interactions [4]. However, no general theoretical agreement exists connecting the symmetry of spin structures, the number of order-parameter components, and the range of interaction with the expected critical behavior and in particular the order of the phase transition. Furthermore, many authors have demonstrated the difficulties in properly identifying the order of the transition on a ground of high-temperature expansion, scaling, renormalization group transformations, and Monte Carlo simulations (see Ref. [4] and references therein). Roomany and Wyld [12] pointed out that the occurrence of second-order type effects at the weakly first-order transitions can be explained by a comparison of the correlation length ξ with the lattice size L . In the case of the $q = 5$ Potts model's weak first-order transition,

Peczak and Landau [13] have observed pseudocritical exponents close to the conjectured values of the critical indices in the $q = 4$ Potts model.

This paper is concerned with the analysis of numerical data, obtained via an accurate entropic Monte Carlo scheme, on triangular Ising finite systems with nearest-neighbor (J_{nn}) and next-nearest-neighbor (J_{nnn}) antiferromagnetic interactions in ratio $R = J_{nn}/J_{nnn} = 1$. Rastelli et al. [14] have recently presented numerical evidence (for $R = 0.1, 0.5$, and 1.0) that, in the thermodynamic limit, this model undergoes a first-order phase transition, from a layered ordered phase (SAF phase) to a high temperature paramagnetic phase. Here, we will present a more detailed identification of the nature of this transition by looking again at the size dependence of the traditional thermodynamic quantities but also by implementing the Lee-Kosterlitz method [15,16] and detecting the first-order character of the transition via the size-dependence of the free energy barrier. Furthermore, we will improve the original estimates of Rastelli et al. [14] and try to verify the predictions of the finite-size scaling (FSS) theory of first-order transitions, including transition point shifts, thermal, and magnetic anomalies.

The theory of FSS near second-order transitions has a rich and longstanding literature [17], starting with the pioneering works of Fisher [18] and Fisher and Barber [19]. This theory has been extended to first-order transitions [4,15,16,20,21,22,23] and FSS and renormalization group methods have proven to be very useful tools for the study of first- and second-order phase transitions [15,16,17,18,19,20,21,22,23,24,25]. Our attempt here to elucidate the distinctive first-order features of the present model, by an extensive numerical study, will closely follow previous analogous studies carried out on the $q = 5, q = 8$, and $q = 10$ Potts model [15,16,21,26,27]. In these studies the existing theories of first-order transitions have been tested and verified but several important aspects have not been thoroughly clarified, especially in the cases of weak first-order transitions. Not only the demonstration of a weak first-order transition is more difficult but also strong finite-size effects may obscure the true asymptotic behavior [16] and some theoretical predictions may not be met even at quite large lattices (since the correlation length may be very large). In such cases, it is very difficult to discriminate between wrong phenomenological expectations and correct theoretical predictions. Therefore, comparisons of different models and alternative studies may provide useful information and a better understanding of finite-size effects, something that is necessary for the correct interpretation of the numerical data and the verification of the theories. The present model, showing a weak first-order phase transition, offers the opportunity of such a contrasting test with the well-studied cases of the Potts model.

Our interest in the present model stems from our recent studies on the analogous square SAF model [28,29], which is again an Ising model on the square lattice with nearest-neighbor (J_{nn}) and next-nearest-neighbor (J_{nnn}) antifer-

romagnetic interactions. The ground state of the square SAF model is four-fold degenerate and consists of the arrangements in which ferromagnetic rows (columns) alternate with opposite oriented spins. In the square model the SAF order can be obtained in both cases of a ferromagnetic or an antiferromagnetic nearest-neighbor coupling (for its $T = 0$ phase diagram see Refs. [7,30,31]). Similarly, the present triangular SAF model, with antiferromagnetic interactions in ratio $R = J_{nn}/J_{nnn} = 1$, has a six-fold degenerate ground state and consists of the six arrangements in which ferromagnetic lines alternate with opposite oriented spins in the three lattice directions ($T = 0$ phase diagrams are given in Refs. [5,9]). The Hamiltonian that governs these systems, in zero-field, is

$$\mathcal{H} = J_{nn} \sum_{\langle i,j \rangle} \sigma_i \sigma_j + J_{nnn} \sum_{\langle i,j \rangle} \sigma_i \sigma_j, \quad (1)$$

where here both nearest-neighbor (J_{nn}) and next-nearest-neighbor (J_{nnn}) interactions will be assumed to be positive (antiferromagnetic). This Hamiltonian has been studied also in $d = 3$ FCC lattices and evidence for both first- and second-order phase transitions have been presented [4,6], although the distinction of the order of the transition was difficult in that case too.

The square model, governed by Eq. (1), develops at low temperatures SAF order for $R > 0.5$ and several early studies [7,30,31,32,33,34,35], mainly based on importance sampling [36,37,38,39,40], have suggested that this system possess anomalous exponents and a non-universal critical behavior with exponents depending on the coupling ratio R . However, despite this early accepted scenario, there has been recently renewed interest and some attempts to re-examine the behavior of this model appeared. In several papers Lopez et al. [41,42,43] have used the cluster variation method (CVM) to study this model, concluding that the system undergoes a first-order transition for a particular range of the coupling ratio R ($R = 0.5 - 1.2$). On the other hand, this different scenario - predicting first-order transitions between ordered and disordered phases followed by continuous transitions outside the first-order region - has now been seriously questioned by the present authors, who have presented very strong evidence [28] for the case $R = 1$ that points out a well-obeyed second-order scaling behavior. The Buzano and Pretti [44] attempt to verify the scenario of Lopez et al. [41,42,43], by including an additional 4-body coupling, and using again the CVM, has revealed a further peculiar inadequacy of the CVM. The limiting case ($J_{nn} = 0$), where the exact solution of the Baxter model [45] applies, was also predicted by the CVM to undergo a first-order transition, in contradiction to the exact solution.

The above introduction describes a rather controversial situation on the class of models with antiferromagnetic ground-state arrangements. Therefore, it is of interest to follow closely the previous FSS analysis applied to the Potts mod-

els and study in more detail the triangular SAF model. In this case, we will insist that this system undergoes a genuine, but weak, first-order transition, as originally predicted by Rastelli et al. [14]. Having a six-fold degenerate ground state arrangement, this model will be shown to produce first-order characteristics that lie between the $q = 5$ and $q = 6$ Potts model. The rest of the paper is organized as follows. In the next Section we outline an extensive entropic sampling program. This program goes beyond our previous practice in other applications [46,47,48,49] and is based on (i) the Wang-Landau (WL) method [50], (ii) our dominant energy restriction (CrMES) scheme [46], and (iii) a second-stage improvement that combines the WL [50], the Lee entropic [51,52], and the broad histogram (BH) [53] or transition matrix [54] methods. In Section 3 we shall review all necessary theoretical aspects of first-order transitions that are then used for the analysis of our numerical data. The free energy barrier method of Lee and Kosterlitz [15,16], used in the literature for the identification of a first-order transition, is discussed in subsection 3.1.1, while the size-dependence of thermal properties derived from the well-known double Gaussian approximation is summarized in subsection 3.2. Finally, some new transition points derived from the number-of-phases parameter [26,27] are presented in subsection 3.3. Section 4 presents the analysis of our numerical data. In subsection 4.1 we make use of several alternative methods for the estimation of the transition temperature presenting a detailed analysis of the new transition points derived from the number-of-phases parameter and a discussion on their conjectured exponentially small shift behavior. In subsection 4.2 we explore our data for the energy cumulants and the magnetic susceptibility, emphasizing on the examination of the higher-order corrections predicted by the double Gaussian approximation. The characteristic values of the energy cumulants, i.e. the coefficient of the dominant diverging term of the specific heat and the limiting values of the second- and fourth-order energy cumulants are determined and the corresponding theoretical predictions are critically discussed. This serves as a useful self-consistency test of our numerical data but also of the theoretical predictions. Finally, our conclusions are summarized in Section 5.

2 Numerical approach

Computer simulations based on Monte Carlo sampling methods have increased dramatically our understanding of the behavior of systems of classical statistical mechanics. The Metropolis method and its variants were for many years the main tools in condensed matter physics and critical phenomena [36,37,38,39,40]. However, for complex systems, effective potentials may have competing minima, or a rugged landscape, becoming more pronounced with increasing system size. In such cases, the traditional methods become completely inefficient, since

they cannot overcome such barriers and cross from one basin to another in the state space. On the other hand, a large number of “generalized ensemble” methods have been proposed to overcome such troubles [39,40,50,51,52,53,54,55,56,57,58,59,60,61,62,63]. One important class of these methods emphasizes the idea of directly sampling the energy density of states (DOS) and may be called entropic sampling methods [39]. In an entropic sampling method, instead of sampling microstates with probability proportional to $e^{-\beta E}$, we sample microstates with probability proportional to $[G(E)]^{-1}$, where $G(E)$ is the DOS, thus producing a “flat energy histogram”. The prerequisite for the implementation of the method, is the DOS information of the system, a problem that can now be handled in many adequate ways. Over the last two decades, there have been a number of interesting approaches addressing this problem. The most remarkable examples are the Lee entropic [51,52], the multicanonical [55,56], the BH [53], the transition matrix [54], and the WL [50] methods. In particular, the WL algorithm [50] has been one of the most refreshing improvements in Monte Carlo simulation schemes and has been already applied to a broad spectrum of interesting problems in statistical mechanics and biophysics [64].

Recently, the present authors have introduced [46,47] a dominant energy subspace implementation of the above entropic methods, called critical minimum energy subspace (CrMES) method. The main idea is a systematic restriction of the energy space with increasing lattice size. The (WL) random walk takes place in the appropriately restricted energy space and this restriction produces an immense speed up without introducing observable errors. For the temperature range of interest, that is the range around a critical or, for the present model, a first-order transition point, this scheme may be used to determine all finite-size thermal anomalies from the final accurate DOS of the WL scheme. A further simplification, for the determination of the magnetic finite-size anomalies, was suggested [47] by using the WL approach as a one-run entropic strategy. In this CrMES WL-entropic sampling method the magnetic properties are obtained by recording appropriate histograms in the high levels (or final levels) of the WL process. It was argued and numerically verified that these high levels, in which the detailed balanced condition is quite well satisfied, give good approximations for the microcanonical estimators, necessary for the evaluation of other properties, besides the thermal ones, of the statistical system. The method was efficiently combined with the N-fold way [37,47,65,66] in order to improve statistical reliability, but also to produce BH estimators, from the same high levels, for an additional calculation of the DOS.

Let us now outline the main ingredients and equations used in the above described implementation. The approximation of canonical averages, in a temperature range of interest, is as follows:

$$\langle Q \rangle = \frac{\sum_E \langle Q \rangle_E G(E) e^{-\beta E}}{\sum_E G(E) e^{-\beta E}} \cong \frac{\sum_{E \in (E_1, E_2)} \langle Q \rangle_{E, WL} \tilde{G}(E) e^{-\beta E}}{\sum_{E \in (E_1, E_2)} \tilde{G}(E) e^{-\beta E}}. \quad (2)$$

The restricted energy subspace (E_1, E_2) is carefully chosen to cover the temperature range of interest without introducing observable errors. The micro-canonical averages $\langle Q \rangle_E$ are determined from the (E, Q) -histograms (denoted by $H_{WL}(E, Q)$), which are obtained during the high levels of the WL process

$$\langle Q \rangle_E \cong \langle Q \rangle_{E,WL} \equiv \sum_Q Q \frac{H_{WL}(E, Q)}{H_{WL}(E)}; \quad H_{WL}(E) = \sum_Q H_{WL}(E, Q) \quad (3)$$

and the summations run over all values generated in the restricted energy subspace (E_1, E_2) . Finally, the approximate DOS used in Eq. (2) is the final “most accurate” DOS generated via the WL iteration [$\tilde{G}(E) = G_{WL}(E)$] or alternatively from the accumulated BH approximation [$\tilde{G}(E) = G_{BH}(E)$]. The initial modification factor of the WL process is taken to be $f_1 = e = 2.718\dots$ and, as usual, we follow the rule $f_{j+1} = \sqrt{f_j}$ and a 5% flatness criterion [46,47]. Details on the N-fold implementation can be found in Refs. [47,49,65,66]. As mentioned above, the recording of the appropriate histograms takes place in the high levels ($j = 18 - 26$) of the WL process, where the incomplete detailed balance condition has no significant effects.

The CrMES restriction may be defined by requesting a specified accuracy on a diverging specific heat (and/or on a diverging susceptibility) [47]. Alternatively, the energy density function may be used to restrict the energy space. This latter restriction is very simple for presentation reasons (see below) but we always use the original recursion method described in Ref. [46], which from our experience produces the most accurate and safe location of the dominant energy subspace. Consider a temperature of interest T_L^* and let \tilde{E} be the value maximizing the probability density, at this temperature. The end-points (\tilde{E}_\pm) of the dominant energy subspaces may be located by the above mentioned simple energy density function condition

$$\tilde{E}_\pm : \frac{P_{\tilde{E}_\pm}(T_L^*)}{P_{\tilde{E}}(T_L^*)} \leq r, \quad (4)$$

where r is chosen to be a small number, independent of the lattice size (i.e. $r = 10^{-6}$). Similarly, let \tilde{M} be the value maximizing the order-parameter density at some pseudocritical temperature, for instance the pseudocritical temperature of the susceptibility ($T_L^* = T_{L,\chi_{max}}^*$). Then, the end-points (\tilde{M}_\pm) of the dominant magnetic subspaces may be located by a similar condition

$$\tilde{M}_\pm : \frac{P_{\tilde{M}_\pm}(T_L^*)}{P_{\tilde{M}}(T_L^*)} \leq r. \quad (5)$$

The finite-size extensions of the above dominant energy and order-parameter

subspaces satisfy respectively the scaling laws of the specific heat and susceptibility with exponents α/ν and γ/ν , respectively [28,29,46,47].

The performance limitations of entropic methods, such as the WL random walk and the reduction of their statistical fluctuations have recently attracted considerable interest [52,67,68]. For the CrMES entropic scheme, presented above, comparative studies using various implementations and the Metropolis algorithm were presented in Refs. [46,47] for the $d = 2$ and $d = 3$ Ising models and also in Refs. [28,29] for the square SAF model. In particular, the effects of the used range of the WL iteration levels on the magnetic properties of the system and also the effect of some refinements of the WL algorithm were discussed. However, for large systems statistical fluctuations significantly increase and their reduction demands, as usually, multiple measurements, i.e. carrying out many WL random walks. The recordings of the (E, Q) -histograms in the high levels of the WL iteration process will in general produce quite accurate estimates for the magnetic or other properties, but it should be noted that this accuracy may well depend on the lattice sizes used but also on the particular model simulated. From our experience, all ingredients of the entropic schemes should be tested and treated with caution. There are, for instance, several ideas in the literature for reducing the modification factor of the WL process but also for the proper use, i.e. recording enough statistics, of the histogram-flatness criterion of the WL method [47,50,52,68].

Taking all these into account, we first applied a multi-energy-range approach [50] using the one-run entropic scheme of Ref. [47], recording the (E, M) -histograms only in the final levels $j = 18 - 26$ of the WL process. For all lattice sizes ($L = 30, 40, \dots, 100, 120, 140, 160, 200, 240, 360$ and 480) this simulation was repeated for 10 independent random walks and averages of the resulting DOS and histograms were constructed. These time-demanding simulations have been greatly facilitated by the dominant energy subspace restriction applied. Even by using an $r = 10^{-6}$ accuracy level, we had to simulate only a small part of the order of 4 – 5% of the energy spectrum for the larger lattices. For $L = 240$ we determined the DOS for about 5400 energy levels (4.7%), which is about 10% wider than the resulting dominant subspace of 5000 energy levels. For $L = 480$ we carried out the simulation in a subspace of 19000 energy levels (4%) and the resulting dominant subspace was about 15500 energy levels (3.36%). These numerical data were used to observe the first-order nature of the present model and in fact the resulting evidence was decisively supporting the first-order character of the transition (note that Figs. 1 and 2 in the next Section are using also these data). However, due to the first-order character the statistical fluctuations for the present model were rather large, compared to other simpler models studied earlier by the same scheme [28,46,47,48]. Accordingly we have carried out a second-stage entropic sampling scheme only for the lattices $L = 40, \dots, 240$. In this scheme we performed two parallel random walks, one using the $j = 26$ modification factor of the WL method (WL-walk)

and the other using the Lee correction [39,51,52] of the DOS (Lee-walk). The total duration of this process was set equal to $10 \times \tau_{26}$, where τ_{26} is the time needed in the original scheme for the saturation of histogram fluctuations [52] of the WL scheme at the level $j = 26$. Details of these additional simulations are given below.

The second-stage simulation was repeated three times for each lattice size, every time starting with a different DOS, selected from our first one-run approach. In time intervals equal to the time-unit τ_{26} , the resulting DOS's from the two parallel walks (WL-walk and Lee-walk) were recorded, as were also recorded the corresponding “microcanonical estimators” for the application of the BH or transition matrix methods. To continue in the next time-step (of duration τ_{26}) we used for both parallel walks the time-accumulated average DOS of the Lee-walk. Of course, this practice is one of many other possibilities and ideas for “refreshing” the DOS, that could be used to continue the further refinement of the DOS via a WL-modification ($j = 26$) or via a Lee-adjustment [51,52]. One can even mix the DOS's of the two parallel walks and/or combine with the DOS's resulting from the BH or transition matrix methods to continue the process (such an example was considered by Shell et al. in Ref. [64]). At the end of the process, we have observed the time development of various thermal properties of the system at some convenient temperatures, for instance the specific heat and fourth-order cumulant pseudotransition temperatures, as well as at a temperature close to the bulk transition temperature ($T_c = 1.80845$). The inspection of their time-behavior verified the accuracy of our original estimates and convinced us that the above described practice yields a steady improvement of the time-accumulated average DOS of all involved methods. For large lattices, the recorded during the WL-walk “microcanonical estimators”, for the application of the BH method, appeared to suffer from some “odd fluctuations”, possibly due to a weak violation of the detailed balance condition, that separated their various thermal estimates from all other estimates obtained from the other involved methods. Although these “odd fluctuations” were within the error-range, we have excluded the corresponding estimates from our thermal averages and we have also used only the (E, M) -histograms recorded via the Lee-walk for the further refinement of our susceptibility estimates. The new averages were used as refined estimates of all properties studied and are presented in our figures using the range $L = 40 - 240$.

Closing this Section, let us consider two different definitions for the order-parameter of the model under study. First, with the help of four sublattices of the SAF ordering one may define a two-component order-parameter and finally use its root-mean-square (*rms*) [34]

$$M^{(1)} = \{M_1 + M_2 - (M_3 + M_4)\} / 4$$

$$M^{(2)} = \{M_1 + M_4 - (M_2 + M_3)\} / 4$$

$$M^{(rms)} = \sqrt{(M^{(1)})^2 + (M^{(2)})^2}. \quad (6)$$

An alternative, and numerically more convenient, definition will also be considered from the sum of the absolute values of the four sublattice magnetizations

$$M = \sum_{i=1}^4 |M_i| / 4. \quad (7)$$

The resulting behavior is very similar and in particular the finite-size extensions of the resulting CrMMS completely coincide. Therefore, for large lattices only the second order-parameter was used in order to minimize computer memory requirements. Using now the above definition for the order-parameter we may also define the magnetic susceptibility χ as follows:

$$\chi(L) = \frac{1}{N} \left(\frac{\langle M^2 \rangle - \langle M \rangle^2}{T} \right). \quad (8)$$

3 General aspects of the first-order transition

In general, first-order transitions [4] are characterized by discontinuities of an order-parameter, like the internal energy or the magnetization, in an idealized infinite system. However, in a finite-system, a true phase transition can not occur. Instead, the jump in the order-parameter is smoothed out into a rounded transition which becomes increasingly sharp as the finite dimensions of the system go to infinity. In this case, the aim of FSS theory is to estimate the width and the possible shifts of the rounded transition and to determine the associated scaling functions. In the following subsections we summarize the main difficulties in making a clear distinction between first and second-order transitions and outline useful aspects of the existing theories of first-order transitions.

3.1 On the nature of the phase transition for the triangular SAF model

As pointed out in the introduction, Rastelli et al. [14] considered the triangular model with nearest- and next-nearest-neighbor antiferromagnetic interactions. Using a conventional (Metropolis) Monte Carlo approach, these authors concluded that the phase transition from the ordered phase at low temperatures to the high temperature paramagnetic phase is first-order. The identification of the nature of the transition was based mainly on the clear presence of the

energy double-peaks reported. Additional indications were detected from the behavior of the peaks of the Binder's fourth-order energy cumulant and also from the scaling of the specific heat, the susceptibility, and the corresponding pseudotransition temperatures. From the FSS behavior of the peaks of the Binder's fourth-order energy cumulant they estimated limiting minimum values different from the value of $2/3$ (expected for a continuous transition) which are typically expected for first-order transitions. The shift behavior of the pseudotransition temperatures was also found in agreement with what is expected at a first-order transition ($T^* \approx T_c + bL^{-d}$). However, some problems were encountered mainly with the FSS of the specific heat peaks. The estimated divergences were found in marked difference with the expectations of the FSS theory of first-order transitions. For the case studied here (corresponding to the interaction ratio $R = 1$) the specific heat exponent α/ν ($C^* \approx bL^{\alpha/\nu}$) was estimated to have a value ~ 1.6 instead of the value $d = 2$, which is the common expectation of all existing theories (see below).

A preliminary qualitative comparative study was recently presented by the present authors [29] where the behavior of the present triangular SAF model was contrasted to the analogous square SAF model. In this latter study, the marked difference between thermally driven first- and second-order transitions was illustrated by using the rather traditional method of observing differences in the energy's and order-parameter's cumulant-behavior between the two models. For the triangular model the behavior was indicative of a first-order transition, in agreement with Ref. [14]. For the square model ($R = 1$) the behavior was strongly indicating a second-order critical point [28,29], in disagreement with the mean-field prediction of Lopez et al. [41,42,43] of a first-order transition for $R < 1.2$. Consequently, the presence of the energy double-peaks and the scaling shift behavior L^{-d} , in the case of the triangular SAF model [14,29], are indications of a first-order transition, while the absence of energy double-peaks and the FSS with critical exponents different from the lattice dimensionality, in the case of square SAF model [28,29], are indications of second-order phase transition. However, caution should be paid in both cases to ensure that the lattice size is sufficiently large so that irrelevant fields have scaled away and the observed behavior is the true asymptotic one and not a strong finite-size effect that may cease to exist in the thermodynamic limit. At this point we may recall some already known pitfalls. The existence of the energy double-peaks for the finite lattice Baxter-Wu model [48,69] is a counter-example since this model undergoes a second-order phase transition. Such continuous phase transitions with a convex dip in the microcanonical entropy, including the Baxter-Wu model and the $q = 4$ Potts model in two dimensions, have been discussed recently by Behringer and Pleimling [70]. In these cases the pseudosignatures of "first-order transitions" are finite-size effects. Similarly the apparent "first-order transition" observed in the fixed magnetization version of the Ising model is also a finite-size effect [71,72,73] and it has been shown that this "transition" ceases to exist in the thermody-

namic limit.

Hence, in order to provide strong evidence and to elucidate the distinctive features for models undergoing first-order transitions, accurate and detailed numerical studies are necessary. Such studies have been carried out on the $q = 5$, $q = 8$, and $q = 10$ Potts model and most of the existing theories have been tested and verified using this model [15,16,21,26,27]. The demonstration of the first-order transition features is more difficult, as should be expected, for weak transitions (the $q = 5$ Potts model is a well-known example) since in these cases the correlation length is relatively large and strong finite-size effects may obscure the true asymptotic behavior [16]. The present extensive numerical study, is an attempt to repeat some of these tests on the triangular SAF model, which as will be seen is an interesting weak first-order transition. Our accurate numerical data will permit us to adequately determine the features of the first-order transition of the model, to make interesting comparisons with previous studies, and to draw conclusions related to the applicability of the existing FSS theories.

3.1.1 *The Lee-Kosterlitz method and the latent heat of the transition*

We proceed in interpreting our numerical data using the free energy barrier method proposed by Lee and Kosterlitz [15,16]. With this method one may unambiguously identify the order of the transition and also evaluate the latent heat of the transition. By computing the energy distribution at various temperatures, we locate a pseudotransition temperature T_h , at which the two equal-height peaks of the energy distribution are observed. These two peaks are located at the values of the energies per site $e_o(L) = E_o(L)/L^d$ and $e_d(L) = E_d(L)/L^d$, corresponding to the ordered and disordered states respectively, and are separated by a minimum at $e_{min}(L) = E_{min}(L)/L^d$. Following Lee and Kosterlitz [16], the free energy barrier is defined with the help of the microcanonical free energy [16,27], $F(e, L) \equiv -\ln P(e, L)$, where $P(e, L)$ is the energy distribution at the pseudotransition temperature T_h . At a first-order transition the microcanonical free energy is assumed to have an expansion of the form

$$F(e, L) = L^d f(e) + L^{d-1} f_\sigma(e) + \dots, \quad (9)$$

where $f(e)$ is the bulk free energy which is a minimum and constant for $e_o \leq e \leq e_d$ and $f_\sigma(e)$ is a surface free energy which has a maximum at e_{min} . The arguments presented by Lee and Kosterlitz [16] suggest the following scaling forms for the finite-size estimates of the locations of the equal-height peaks

$$e_o(L) = e_o - \mathcal{O}(L^{-1}) \quad (10)$$

and

$$e_d(L) = e_d + \mathcal{O}(L^{-1}), \quad (11)$$

where e_o and e_d are the bulk energies of the ordered and disordered states respectively. From the above assumptions for the bulk and surface free energies, it follows that the maximum of the surface energy at e_{min} produces a free energy barrier that scales according to

$$\Delta F(L) = F(e_{min}, L) - F(e_o, L) \sim L^{d-1}. \quad (12)$$

This scaling form has been used as a basic test [15,16,27,74] for detecting a temperature-driven first-order transition, while the predicted scaling behavior [Eqs. (10) and (11)] can be used to extrapolate and obtain the latent heat of the transition $\Delta e = e_d - e_o$.

Fig. 1 presents the energy distributions for small and large lattice sizes. Although, for the larger lattices the simulation error fluctuations are evident, it is also very clear that with increasing lattice size the barrier between the two peaks is steadily increasing, signaling the emergence of the expected two delta-peak behavior in the thermodynamic limit. Thus, this figure is an effective demonstration of the persistence of the first-order transition. Fig.2(a) is the corresponding illustration, including all lattice sizes studied, of the behavior of the free energy barrier, defined above. It is apparent from this figure that the surface tension, that is the quantity $\Delta F/L = \{k_B T \ln(P_{max}/P_{min})\}/L$, tends to a non-zero value and the attempt to extrapolate by the dotted line gives a value of the order 0.00539(12). Thus, the expectation (12) of the arguments of by Lee and Kosterlitz [16] is well verified. Fig. 2(b) illustrates the L -dependence of the location of the energy density peaks (minima of the free energy) as well as their difference. Again in the scale shown, the expectations described by Eqs. (10) and (11) are well satisfied. Thus, using linear extrapolations in the range of large L , we have estimated the bulk energies $e_o = -1.61784(728)$ and $e_d = -1.48852(565)$, and the latent heat of the transition $\Delta e = e_d - e_o = 0.129(12)$. This is to be compared with the value 0.176(6) estimated by Rastelli et al. [14].

3.2 The double Gaussian approximation

K. Binder and co-workers [20,21,75] introduced the so-called double Gaussian approximation. This assumption concerns the probability distribution of the order-parameter and has become a widely used feature in the theories of first-order transitions. The original approach leading to this approximation

was based on the intuitive extension of the Gaussian approximation of a single phase, which may be theoretically justified by appealing to the central limit theorem. It was argued [20,21,75] that, the distinctive feature of a first-order transition is the coexistence of phases at the transition point and in fact this important observation is the starting point of other theories of first-order transitions [15,16,24,20,21,26,27,75,76,77,78,79,80,81,82,83,84,85]. Ignoring effectively interface effects between domains of different phases, the equilibrium of the phases is described by a superposition of Gaussians centered at different values of the order parameter corresponding to the different coexisting phases.

Furthermore, it was soon realized [15,16] and theoretically [78,79,80,81,82,83,84,85] justified, that the same qualitative picture can be obtained by a more fundamental assumption. The partition function of a large finite system, with periodic boundary conditions, undergoing in the limit $L \rightarrow \infty$ a first-order transition, is well approximated at the transition point as a sum of terms, each describing a separate phase. For temperature-driven first-order phase transitions, in which q equivalent ordered phases coexist at the transition temperature (β_c) with one disordered phase, the dominant contributions in the partition function, separated in contributions from the different coexisting phases, may be written as [16]

$$Z = \sum_{i=1}^{q+1} e^{-\beta_c f_i(\beta_c) L^d}, \quad (13)$$

where $f_i(\beta_c)$ is the free energy per site of the i th phase in the thermodynamic limit. This fundamental relationship is a statement that each phase contributes equally to Z at the transition temperature ($f_i(\beta_c) = f(\beta_c)$). As pointed out by Lee and Kosterlitz [16], the double Gaussian approximation may be obtained by assuming an extension of (13) in the vicinity of T_c and using appropriate temperature Taylor expansions for the free energies $f_i(\beta)$ of the coexisting phases. The probability density for the energy can then be obtained by the inverse Laplace transform of the expanded partition function and, in order $\mathcal{O}(L^{-d})$ in the free energy expansion, one can derive the double Gaussian form

$$P(e) = \frac{e^\Delta}{e^\Delta + e^{-\Delta}} \Phi_G(e; \tilde{e}_o, \sigma_o) + \frac{e^{-\Delta}}{e^\Delta + e^{-\Delta}} \Phi_G(e; \tilde{e}_d, \sigma_d), \quad (14)$$

where $\Phi_G(e; \tilde{e}_i, \sigma_i)$ is the normal distribution with mean $\tilde{e}_i = e_i + C_i(\frac{T_c}{T})(T - T_c)$ and variance $\sigma_i^2 = k_B T_c^2 C_i L^{-d}$. e_i and C_i are the energy and specific heat of the i th bulk phase, derived as appropriate derivatives from the corresponding free energies. Furthermore,

$$\Delta = \frac{1}{2} \ln q + \frac{1}{2} (e_o - e_d) \frac{T_c}{T} (T - T_c) L^d + \frac{1}{4} (C_o - C_d) \left(\frac{T - T_c}{T} \right)^2 L^d, \quad (15)$$

so that the ratio of weights corresponding to the two terms of Eq. (14) satisfies the relation

$$\frac{w_o}{w_d} = e^{2\Delta} = qe^{\beta(f_d - f_o)L^d}. \quad (16)$$

From the above distribution, or in a more straightforward way, by using differentiation of the expanded partition function one can deduce the finite-size behavior of all energy cumulants, as shown by Lee and Kosterlitz [16]. These tedious calculations have been also repeated by Janke [27] and in the following we summarize only the relevant results that have been used in our study of the triangular SAF model. At this point let us emphasize the fact, stated explicitly below, that the double Gaussian approximation predicts, in general, that all finite-size contributions enter in the scaling equations in powers of L^{-d} . The general shift behavior predicted for the various pseudotransition temperatures (denoted collectively as T_i^*) is

$$T_i^* = T_c + bL^{-d}(1 + \mathcal{O}(L^{-d})), \quad (17)$$

where these temperatures correspond to the peaks of various energy cumulants such as those defined below. As noted above, not only the main shift contribution but also the higher-order corrections enter in Eq. (17) only in powers of L^d . Three different energy cumulants have been used in our calculations, the specific heat per site $C(L)$, the second-order cumulant $U_2(L)$, and the Binder's fourth-order cumulant $V_4(L)$. Below we give their definitions and the predicted scaling behavior [16,27] at the corresponding pseudotransition temperature, at which the cumulant peak (maximum or minimum) occurs

$$C(L) = L^{-d} \{ \langle E^2 \rangle - \langle E \rangle^2 \} / T^2 \quad (18)$$

$$C(L)L^{-d}|_{max} = \frac{(e_o - e_d)^2}{4T_c^2} (1 + \mathcal{O}(L^{-d})) \quad (19)$$

$$U_2(L) = \frac{\langle E^2 \rangle}{\langle E \rangle^2} \quad (20)$$

$$U_2(L)|_{max} = \frac{(e_o + e_d)^2}{4e_o e_d} + \mathcal{O}(L^{-d}) \quad (21)$$

$$V_4(L) = 1 - \frac{\langle E^4 \rangle}{3\langle E^2 \rangle^2} \quad (22)$$

$$V_4(L)|_{min} = \frac{2}{3} - \frac{(e_o/e_d - e_d/e_o)^2}{12} + \mathcal{O}(L^{-d}). \quad (23)$$

In the following Section we proceed to test the above scaling laws for the triangular SAF model. In particular, the coefficient of the dominant diverging term of the specific heat and the limiting values of the cumulants U_2 and V_4 , will be determined in two independent ways: (a) by finding their values from convincing fitting assumptions of our peak-data and (b) from the extrapolated values of the energies e_o and e_d (see Fig. 2(b) and Eqs. (10) and (11)) and the above predictions. The proposed comparison will provide a useful self-consistency test of our results but also of the theoretical predictions. It will also assist a critical discussion on the higher-order corrections of the double Gaussian approximation. Noteworthy, that the above leading terms may also be derived heuristically from a simple two-phase model, as shown by Janke [27].

3.3 Number-of-phases parameters and the determination of transition points

Traditionally, the general shift behavior $T^* \approx T_c + bL^{-d}$ has been used for both the identification of a first-order transition and the determination of the transition temperature. However, Borgs and Janke [26] have suggested additional methods facilitating the determination of transition points for systems with periodic boundary conditions. Two such methods will be discussed below and then elaborated in the sequel to observe the behavior of the present first-order transition. In the first method, a parameter is introduced that requires two different finite lattices of volumes $V_1 = L_1^d$ and $V_2 = L_2^d$ respectively. This parameter has been called the number-of-phases parameter [27] and is defined as:

$$N(V_1, V_2; \beta) = \left[\frac{Z_{per}(V_1; \beta)^\alpha}{Z_{per}(V_2; \beta)} \right]^{1/(\alpha-1)}, \quad (24)$$

where α is the volume ratio $\alpha = V_2/V_1 = (L_2/L_1)^d$. The origin of this parameter is the fundamental relationship (13), which is extended, as earlier, in the vicinity of the transition point by introducing [26,27] metastable free energy densities $f_i(\beta)$. These are defined in such a way that are equal to the bulk free energy $f(\beta)$ in the temperature range in which the corresponding phase is a stable phase and strictly larger than $f(\beta)$ when the phase is unstable. The coexistence partition function is now written as [26,27]

$$Z_{per}(V; \beta) = \left\{ \sum_{i=1}^{q+1} e^{-\beta f_i(\beta)V} \right\} \left(1 + \mathcal{O}(V e^{-L/L_o}) \right). \quad (25)$$

A heuristic derivation of the above exponential correction bound has been presented in Ref. [26]. The hypothesis for exponential small shifts, to be discussed in the next Section, derives from the above bound. Eq. (25) and the

assumptions of the behavior of metastable free energy densities may be used to show [27] that the parameter

$$N(\beta) = \lim_{V \rightarrow \infty} Z_{per}(V; \beta) e^{\beta f(\beta)V} \quad (26)$$

is equal to the number of stable phases, which with increasing temperature takes the values q , $q + 1$, and 1. A finite-size approximation of the above parameter will be expected to have a peak at a finite-size transition point ($T_{V/V}$) and the number-of-phases parameter defined in Eq. (24) is a suitable such approximation that may be used to locate the transition point. The condition for the maximum of the parameter of Eq. (24) corresponds to the crossing point of the mean energy functions of the pair of lattices involved and reads as:

$$\alpha \langle E_1 \rangle |_{T_{V/V}} = \langle E_2 \rangle |_{T_{V/V}} \quad \text{or} \quad \langle e_1 \rangle |_{T_{V/V}} = \langle e_2 \rangle |_{T_{V/V}}. \quad (27)$$

The location of the peaks of the parameter (24) can be estimated by a dominant CrMES scheme, such as that followed by the present authors in other applications [28,46,47]. Of course, the restricted energy space scheme should be sufficient for both lattices of the pair in the temperature range of interest, that is in the region of the peaks. We shall use the sequence of pairs of lattices: (40, 80), (50, 100), (60, 120), (70, 140), (80, 160), (100, 200), and (120, 240), with volume ratio $\alpha = 4$ ($L_2 = 2L_1$, $d = 2$). Fig. 3(a) illustrates the behavior which is similar with the behavior presented by Janke [27] for the Potts model.

We now discuss a variant of the above number-of-phases parameter. First, we define a “reduced partition function”. The maximum term, at each temperature, has been factorized and dropped out from the partition function’s sum. Thus,

$$\tilde{Z}(V; \beta) = \sum_{(\tilde{E}_-, \tilde{E}_+)} e^{\tilde{\Phi}(E)}, \quad (28)$$

where $\tilde{E} = \tilde{E}(T)$ is the most probable energy corresponding to the maximum term, and

$$\tilde{\Phi}(E) = S(E) - \beta E - [S(\tilde{E}) - \beta \tilde{E}]. \quad (29)$$

Since the most probable energy has two values at the equal-height temperature (T_h), the above reduction introduces in the above definition microcanonical features of the transition. These features are now carried over to the new ratio

parameter

$$\tilde{N}_\lambda(V_1, V_2; \beta) = \frac{\tilde{Z}(V_1; \beta)^\lambda}{\tilde{Z}(V_2; \beta)}. \quad (30)$$

Let us regard the exponent λ as a free parameter, not necessarily equal to the volume ratio of the two systems ($\alpha = 4$), and observe the resulting behavior. Fig. 3(b) shows the behavior of this new ratio parameter for the case $\lambda = 2$ and the three larger lattice size pairs of the sequence considered above. It can be seen from this figure that by increasing the temperature this parameter shows a first maximum peak (T_{max1}) which resembles the peak of the original number-of-phases parameter. Further increase in the temperature yields, for each pair, two additional very sharp peaks, one minimum (T_{min}) and one maximum (T_{max2}). These two peaks are reflections of the maximum term reduction in the definition (30). The sharp minimum corresponds to the equal-height pseudotransition temperature T_h of the larger lattice, while the sharp maximum corresponds to the equal-height pseudotransition temperature T_h of the smaller lattice. The value of the exponent λ determines the location of the first maximum peak and the sharpness of these graphs. Thus, a similar but less pronounced picture is obtained for the values $\lambda = 3$ and $\lambda = 4$, and it is found that the location of the two new sharp peaks are not notably influenced by the change in the value of the exponent λ . This can be easily understood since the new sharp peaks are in effect properties of the two separated lattices. The peaks of this new ratio can be also be described by an approximate crossing condition, similar to Eq. (27), which may be written as:

$$\lambda(\langle e_1 \rangle - \tilde{e}_1)|_{\tilde{T}} = \alpha(\langle e_1 \rangle - \tilde{e}_1)|_{\tilde{T}}. \quad (31)$$

In the above condition we have neglected the temperature variation of the most probable energy value \tilde{E} . This variation will produce vanishing contributions, as tested also numerically, involving the difference between microcanonical and canonical temperature $[(\partial S_i / \partial E_i)|_{\tilde{E}_i} - \beta]$.

Fig. 4(a) is an illustration of the crossing point of the mean energy functions of a pair of systems ($L_1 = 80, L_2 = 160$) corresponding to the peak of the original number-of-phases parameter (24). In this the behavior of the most probable energies of the pair of systems is also illustrated. Fig. 4(b) presents the temperature behavior of the differences, $\langle e \rangle - \tilde{e}$, of the two characteristic energies for each system of the chosen pair. For the larger lattice the graph corresponding to the double of the difference $\langle e \rangle - \tilde{e}$ is also shown in order to facilitate the illustration of the above crossing relationship (31) for $\lambda = 2$. Noteworthy, that this illustration provides an alternative practical way of locating the equal-height pseudotransition temperature T_h , since at this temperature (inversion point) the corresponding difference changes sign. As we increase the

temperature, the difference curve of the smaller lattice is crossed by the curve of the larger lattice at a point (T_{max1}) corresponding to the first maximum in Fig. 3(b). As can be seen the location of this point (\tilde{T}_λ) depends on the value of the exponent λ and for the value $\lambda = \alpha/2 = 2$, the crossing is deeper and occurs at a lower temperature, than in the case corresponding to $\lambda = \alpha = 4$. This explains why the first maximum peak (T_{max1}) in the case $\lambda = 2$ is more pronounced as mentioned earlier. Finally, the sharp minimum (T_{min}) and the sharp maximum (T_{max2}) in Fig. 3(b) are described by the crossing points corresponding to the inversion points of the larger and smaller lattice respectively and their location is not practically influenced by the value of the exponent λ .

We shall conclude this Section with a brief reference on the second definition of a finite-size transition point introduced by Borgs and Janke [26]. This equal-weight finite-size transition point (T_W) requires data from one lattice only and is the point where the ratio of the total weight of the ordered phases to the weight of the disordered phase approaches q , so that

$$R(V, E) = \sum_{E < E_m} P(E) / \sum_{E \geq E_m} P(E) \equiv \frac{W_o}{W_d}|_{T_W} = q, \quad (32)$$

where E_m may be chosen in various ways and following Refs. [26,27] we will choose it to be the energy of the minimum between the two equal-height peaks at the pseudotransition temperature T_h . As a variant of the above definition, we have attempted to satisfy Eq. (32) using the part of the weights above the minimum between two unequal peaks. The resulting transition points have similar behavior and will not be presented.

4 Analysis of numerical data

4.1 Estimation of the transition temperature

Using our accurate data and various alternative methods we have estimated the transition temperature with an error at most in the fifth significant figure. Our safe estimate is $T_c = 1.8085(1)$ and is an improvement of the three estimates of the order of $T_c = 1.8078(1)$, given originally by Rastelli et al. [14] and close to their magnetic fourth-order cumulant estimate $T_c = 1.8084(1)$. An interface method estimation of this transition point ($T_c = 2.044$) was given by Slotte and Hemmer [86]. Fig. 5(a) presents a first attempt to estimate the transition temperature by a simultaneous fitting on five pseudotransition temperatures. As indicated, in an obvious notation on the graph, these are the equal-height temperature (T_h) and the pseudotransition temperatures corresponding to the peaks of the specific heat, second- and fourth-order energy

cumulants, and finally the peak of the susceptibility. In the first attempt the shift behavior predicted by the double Gaussian approximation has been assumed including also the first shift correction term L^{-2} (i.e. $\mathcal{O}(L^{-d})$). Fig. 5(b) presents a second attempt using now a variant of the above assumption by replacing the shift correction term with an L^{-1} correction. This replacement makes practically no difference in estimating the transition temperature because the dominant shift term is about three orders of magnitudes larger than the next correction in all cases, and the asymptotic behavior has been well reached in the temperature shift behavior. Noteworthy that, if we restrict the fitting attempt in the range $L = 30 - 140$, we will obtain an estimate $T_c = 1.80845(5)$.

Next we present the behavior of the new transition point observables introduced by Borgs and Janke [26], as well as the similar ones introduced and discussed in the last subsection. Although we will not try to further refine the above accurate estimate, it is of interest to illustrate their behavior, show that they lead to the same estimate, and discuss their behavior in comparison with previous studies on the Potts model. Fig. 6(a) illustrates the behavior of the three peaks of the reduced number-of-phases parameter defined in the last Section in Eq. (30) for $\lambda = 2$. The data for the two peaks (T_{max2} and T_{min}) are approaching from above the transition point and coincide in practice with the equal-height temperatures for the smaller and larger lattices respectively, as explained in subsection 3.3. The data for the peaks T_{max1} , which resemble the original peaks of the number-of-phases parameter of Borgs and Janke [26], are also moving steadily to the expected limit and their fitting, using Eq. (17), yields again the estimate $T_c = 1.8085(1)$. Fig. 6(b) collects the behavior of six finite-size transition points and compares them with our estimate for the transition point and also with the estimate $T_c = 1.8078$ of Rastelli et al. [14]. We have included in this figure two transition points depending only on one lattice, namely the equal-height transition point (T_h) and the weight transition point (T_W) defined in Eq. (32). The rest of the shown transition points are the original number-of-phases parameter transition point introduced by Borgs and Janke [26], denoted as $T_{V/V}$, and the left maximum point (T_{max1} or \tilde{T}_λ) of the reduced number-of-phases parameter introduced in this paper for three values of the exponent λ , $\lambda = 2, 3$ and 4 (see the discussion below Eq. (31)). Their limiting behavior is an extra verification of our estimate for the transition temperature.

Borgs and Janke [26] in their Fig. 2, and Janke [27] in his Fig. 11, have illustrated the behavior of the transition points $T_{V/V}$ and the T_W for the Potts model with $q = 5$, $q = 8$, and $q = 10$. As it can be seen from the mentioned figures, the $q = 8$ and $q = 10$ finite-size transition points approach their bulk limit for relatively small lattices. Therefore, these authors have concluded that for strong first-order phase transitions the exponential bound in Eq. (25) provides a natural explanation of the observed “exponentially small” shifts

with respect to the infinite-volume transition point. For the weak first-order transition of the $q = 5$ Potts model, the weight transition point T_W can also be seen from the mentioned figures to have reached the bulk limit even for the smallest lattice size $L = 20$. However, the number-of-phases parameter transition points $T_{V/V}$ did not obey this exceptional behavior, but rather its shift behavior resembled the shift behavior of the traditional pseudotransition temperatures, i.e. an L^{-d} shift. Accordingly, Janke [27] has raised also the question of a possible fortuitous cancellation and has suggested the interest to the investigation of these exponentially small shifts in other weak first-order transitions. Fig. 6(b) provides an example showing that for the present weak first-order transition the expectation for exponentially small shifts is not verified for both transition points T_W and $T_{V/V}$. Their behavior differs appreciably from their bulk limit and the reduced number-of-phases parameter for the value $\lambda = 4$ yields the smaller shifts, smaller than that of the natural number-of-phases parameter.

4.2 Behavior of the energy cumulants and the magnetic susceptibility

It is well known that the FSS behavior of the specific heat, and in particular its peak-scaling behavior, may be obscured by the presence of unknown correction terms and the extraction of the scaling exponent may be a numerically indecisive and difficult task [39,40,74]. The accuracy of numerical data is then of crucial importance [40]. This unpleasant problem may also occur in the estimation of other related energy cumulants. For the present model such problems were obviously encountered by Rastelli et al. [14]. Their estimation of the specific heat exponent α/ν ($C^* \approx bL^{\alpha/\nu}$) was found in clear disagreement (estimated to have a value ~ 1.6) with the theoretically expected value $\alpha/\nu = d = 2$. Since the evidence for the present first-order transition is now overwhelming we will adopt the generally accepted theoretical prediction for the leading contribution to the specific heat divergence. Thus, we shall fix the value of the exponent $\alpha/\nu = d = 2$ and we will examine whether there is a stable form of corrections terms that is compatible with our accurate data in the peak-region.

Fitting our numerical data from the first 10 WL runs in various L -ranges, we found that the simple correction term of the form cL^{-1} , instead of cL^{-2} predicted by the double Gaussian approximation, yielded stable fittings in all the L -ranges tried, from $L = 30$ to $L = 480$. The very small variations in the involved coefficients (5% or less) of the fitting attempts are, of course, strong indications in favor of this otherwise ad hoc assumption. Fig. 7 shows that even the remote L -ranges: $L = 30 - 140$ and $L = 100 - 480$ produce 4% deviation in the coefficient of the leading term and only 1% in the coefficient of the assumed correction term. Fig. 8 provides further strong support

in favor of the above assumption using our second-stage refined data in the range $L = 40 - 240$. This figure present simultaneous fittings of the specific heat data not only at its pseudotransition temperature but also in the other pseudotransition temperatures corresponding to the peaks of the other energy cumulants, the peak of the magnetic susceptibility and the equal-height transition point. Noteworthy, that such a simultaneous fitting approach, quite easily implemented within our entropic scheme, would be a rather demanding task in a traditional importance sampling Monte Carlo scheme. In this way we are probing systematically the FSS behavior of the divergence of the specific heat in a wide region around its peak. Fig. 8(a) illustrates the fitting attempt based on the above mentioned (cL^{-1}) assumption and Fig. 8(b) shows a remarkable decline from the double Gaussian prediction (cL^{-2}). The double Gaussian prediction does not correctly describe the correction term and this is reflected in the resulting very large χ^2 error value which is about 35 times larger than the value corresponding to the well obeyed correction term (cL^{-1}). Let us now use the corresponding coefficients of the dominant divergences for the peaks of the specific heat to compute the resulting values for the latent heat and compare these values with the value obtained earlier from the extrapolations of Fig. 2(b), based on the proposal of Lee and Kosterlitz [16] and described in Eqs. (10) and (11). The resulting values for the latent heat from the fittings in Fig. 8 are in the range $0.121 - 0.133$ and $0.143 - 0.163$ respectively. These values should be compared with the value $0.129(12)$, see also Table 1 below, obtained from the extrapolated values of e_o and e_d .

An analogous behavior is observed in the FSS behavior of the other two energy cumulants. Fig. 9(a) shows in the same graph fitting attempts using the data for the minima of the Binder's fourth-order cumulant presuming again the two different assumptions for the correction terms (bL^{-2} and bL^{-1}). As can be seen from this figure the double Gaussian prediction fails again to correctly describe the correction term. The resulting very large χ^2 error value is now 135 times larger than the value corresponding to the simple correction term of the form bL^{-1} . Furthermore, the limiting value corresponding to the assumption using the double Gaussian correction term is $0.66259(40)$ for the L -range shown, which differs appreciably from the value $0.66435(33)$, obtained from Eq. (23) and the extrapolated values of e_o and e_d given in Table 1. On the other hand the limiting value resulting from a leading correction of the form L^{-1} gives $0.66465(25)$ for the L -range shown, as illustrated in Fig. 9(b), and favors an expansion starting with the term bL^{-1} . Fig. 10 repeats the above comparison for the second-order cumulant U_2 . The expansion starting with the term bL^{-1} is surprisingly well obeyed, while the double Gaussian behavior is inconsistent. The limiting value obtained from double Gaussian correction term is $1.00308(25)$ in clear disagreement with the value $1.00174(25)$ obtained from Eq. (21) and the extrapolated values of e_o and e_d , while the proposed expansion in Fig. 10(b) gives the value $1.00163(15)$ quite in agreement with the also approximate estimate $1.00174(25)$.

Table 1 summarizes the estimates for the above thermal characteristics including also the corresponding exact values [16,27,87,88] for the cases $q = 10, 8, 6$ and $q = 5$ of the Potts model. The estimates for the triangular SAF model with $R = 1$ interpolate between the values of the $q = 5$ and $q = 6$ Potts model. Therefore, we have called the present transition a weak first-order transition. It appears that the six-fold degeneracy of the ground state of the present model plays an important role in determining the weakness of the transition, and possibly the occurrence of its first-order character. Finally, let us turn to the behavior of the magnetic susceptibility χ . We present in Fig. 11 the divergence of the susceptibility χ at the five pseudocritical temperatures T_i^* , using again the two types of corrections, i.e. an L^{-1} (Fig. 11(a)) and an L^{-2} (Fig. 11(b)), respectively. The solid lines are simultaneous fitting attempts, using the power laws shown in the figures. Comparing Figs. 11(a) and (b) we see that, although one can not just by inspection differentiate between an L^{-1} and an L^{-2} correction term, χ^2 is smaller for the former correction.

5 Conclusions

The triangular Ising model with nearest- and next-nearest-neighbor antiferromagnetic interactions has been studied and its first-order transition features have been clarified, when the interaction ratio is $R = 1$. We have outlined the most important aspects of the existing theories of first-order transitions and we have tested on this model some basic hypothesis from these theories, comparing our results and findings with previous work on the Potts model. Our numerical data have been used to obtain accurate estimates for all the thermal characteristics of the present weak first-order transition. All the generally accepted predictions of the finite-size scaling theory for first-order transitions, concerning transition point shifts, thermal, and magnetic anomalies, have been well verified for the present model.

However, two of our findings for this model are not compatible with some theoretical or phenomenological expectations. The first of these concerns the behavior of the new transition point observables introduced by Borgs and Janke [26] and also some similar transition points introduced in this paper. These finite-size transition points are suitable finite-size approximations of the fundamental number-of-phases parameter and it has been theoretically argued [16,27] that should be expected to obey exponentially small shifts. This expectation is not verified for the present weak first-order transition.

Finally, we have shown that the well-known double Gaussian approximation does not describe correctly the higher correction terms for all energy cumulants of the present model. It appears that the first correction term in the expansions of energy cumulants is of the form $L^{-d+1}(= L^{-1})$ and not of the

form $L^{-d}(= L^{-2})$, expected from the double Gaussian approximation. Lee and Kosterlitz [16] have pointed out the inadequacy of the Gaussian approximation to produce shifts in the locations of the energies of the equal-height peaks in agreement with those described by Eqs. (10) and (11), which are rather well observed in simulations (see Ref. [16] and Fig. 2(b)). In fact the shortcomings of the Gaussian behavior has been critically discussed in the early work of Challa et al. [21]. Our analysis is therefore suggesting again the need for a more realistic theory. It is tempting to assume that the attempted here and well obeyed expansions for the energy cumulants, starting with the correction term bL^{-1} , may have their origin in the neglected domain wall corrections and could have the same explanation with the existing puzzling situation concerning the shift behavior of the free energy minima pointed out by Lee and Kosterlitz [16].

Acknowledgements

This research was supported by the Special Account for Research Grants of the University of Athens under Grant Nos. 70/4/4071. N.G. Fytas would like to thank the the Alexander S. Onassis Public Benefit Foundation for financial support.

References

- [1] W. Selke, in Phase Transitions and Critical Phenomena, edited by C. Domb and J.L. Lebowitz, Academic Press, London, 1992, vol. 15.
- [2] D. Lawrie, S. Sarbach, in Phase Transitions and Critical Phenomena, edited by C. Domb and J.L. Lebowitz, Academic Press, London, 1992, vol. 9.
- [3] L. Onsager, Phys. Rev. 65 (1944) 117; R.J. Baxter, Exactly solved models in statistical mechanics, Academic Press, London, 1982; B. McCoy, T. Wu, The Two Dimensional Ising Model, Harvard University Press, Cambridge, 1972.
- [4] K. Binder, Rep. Prog. Phys. 50 (1987) 783.
- [5] Y. Tanaka, N. Uryû, J. Phys. Soc. Jpn. 39 (1975) 825.
- [6] M.K. Phani, J.L. Lebowitz, M.H. Kalos, Phys. Rev. B 21 (1980) 4027.
- [7] J. Oitmaa, J. Phys. A 14 (1981) 1159.
- [8] M.J. Velgakis, J. Oitmaa, J. Phys. A 21 (1988) 547.
- [9] D.P. Landau, Phys. Rev. B 27 (1983) 5604.

- [10] M. Bretz, Phys. Rev. Lett. 38 (1977) 501.
- [11] E. Domany, M. Schick, J.S. Walker, R.B. Griffiths, Phys. Rev. B 18 (1978) 2209.
- [12] H.H. Roomany, H.W. Wyld, Phys. Rev. B 23 (1981) 1357.
- [13] P. Peczak, D.P. Landau, Phys. Rev. B 39 (1989) 11932.
- [14] E. Rastelli, S. Regina, A. Tassi, Phys. Rev. B 71 (2005) 174406.
- [15] J. Lee, J.M. Kosterlitz, Phys. Rev. Lett. 65 (1990) 137.
- [16] J. Lee, J.M. Kosterlitz, Phys. Rev. B 43 (1991) 3265.
- [17] For a review of FSS see M. N. Barber, in Phase Transitions and Critical Phenomena, edited by C. Domb and J.L. Lebowitz, Academic, New York, 1983, Vol. 8. See also K. Binder, *ibid.*, Vol. 8.
- [18] M.E. Fisher, in Critical phenomena, Proc. Enrico Fermi International School of Physics, ed. M.S. Green, Academic Press, New York, 1971, Vol. 51.
- [19] M.E. Fisher, M.N. Barber, Phys. Rev. Lett. 28 (1972) 1516.
- [20] K. Binder, D.P. Landau, Phys. Rev. B 30 (1984) 1477.
- [21] M.S.S. Challa, D.P. Landau, K. Binder, Phys. Rev. B 34 (1986) 1841.
- [22] V. Privman, in Finite-size scaling and numerical simulation of statistical systems, ed. V. Privman, World Scientific, Singapore, 1990.
- [23] K. Binder, in Computational methods in field theory, eds. H. Gausterer, C.B. Lang, Springer, Berlin, 1992, p. 59.
- [24] M.E. Fisher, A.N. Berker, Phys. Rev. B 26 (1982) 2507.
- [25] B. Nienhuis, A.N. Berker, E.K. Riedel, M. Schick, Phys. Rev. Lett. 43 (1979) 737.
- [26] C. Borgs, W. Janke, Phys. Rev. Lett. 68 (1992) 1738.
- [27] W. Janke, Phys. Rev. B 47 (1993) 14757.
- [28] A. Malakis, P. Kalozoumis, N. Tyraskis, Eur. Phys. J. B 50 (2006) 63.
- [29] A. Malakis, P. Kalozoumis, N.G. Fytas, Rev. Adv. Mater. Sci. (in press).
- [30] D.P. Landau, K. Binder, Phys. Rev. B 31 (1985) 5946.
- [31] K. Minami, M. Suzuki, J. Phys. A 27 (1994) 7301.
- [32] M.P. Nightingale, Phys. Lett. A 59 (1977) 486.
- [33] R.H. Swendsen, S. Krinsky, Phys. Rev. Lett. 43 (1979) 177.
- [34] K. Binder, D.P. Landau, Phys. Rev. B 21 (1980) 1941.
- [35] D.P. Landau, Phys. Rev. B 21 (1980) 1285.

- [36] N. Metropolis, A.W. Rosenbluth, M.N. Rosenbluth, A.H. Teller, Teller, J. Chem. Phys. 21 (1953) 1087.
- [37] A.B. Bortz, M.H. Kalos, J.L. Lebowitz, J. Comput. Phys. 17 (1975) 10.
- [38] K. Binder, Rep. Prog. Phys. 60 (1997) 487.
- [39] M.E.J. Newman, G.T. Barkema, Monte Carlo Methods in Statistical Physics, Clarendon Press, Oxford, 1999.
- [40] D.P. Landau, K. Binder, A Guide to Monte Carlo Simulations in Statistical Physics, Cambridge University Press, Cambridge, 2000.
- [41] J.L. Morán-Lopéz, F. Aguilera-Granja, J.M. Sanchez, Phys. Rev. B 48 (1993) 3519.
- [42] J.L. Morán-Lopéz, F. Aguilera-Granja, J.M. Sanchez, J. Phys. C 6 (1994) 9759.
- [43] E. López-Sandoval, J.L. Moran-Lopez, F. Aguilera-Granja, Solid State Commun. 112 (1999) 437.
- [44] C. Buzano, M. Pretti, Phys. Rev. B 56 (1997) 636.
- [45] R.J. Baxter, Ann. Phys. (N.Y.) 70 (1972) 193.
- [46] A. Malakis, A. Peratzakis, N.G. Fytas, Phys. Rev. E 70 (2004) 066128.
- [47] A. Malakis, S.S. Martinos, I.A. Hadjiagapiou, N.G. Fytas, P. Kalozoumis, Phys. Rev. E 72 (2005) 066120.
- [48] S.S. Martinos, A. Malakis, I.A. Hadjiagapiou, Physica A 352 (2005) 447.
- [49] A. Malakis, N.G. Fytas, Phys. Rev. E 73 (2006) 016109.
- [50] F. Wang, D.P. Landau, Phys. Rev. Lett. 86 (2001) 2050; Phys. Rev. E 64 (2001) 056101; B.J. Schulz, K. Binder, M. Muller, D.P. Landau, *ibid.* 67 (2003) 067102.
- [51] J. Lee, Phys. Rev. Lett. 71 (1993) 211.
- [52] H.K. Lee, Y. Okabe, D.P. Landau, Comput. Phys. Commun. 175 (2006) 36.
- [53] P.M.C. de Oliveira, T.J.P. Penna, H.J. Herrmann, Braz. J. Phys. 26 (1996) 677.
- [54] J.-S. Wang, T.K. Tay, R.H. Swendsen, Phys. Rev. Lett. 82 (1999) 476; J.-S. Wang, R.H. Swendsen, J. Stat. Phys. 106 (2002) 245.
- [55] B.A. Berg, T. Neuhaus, Phys. Lett. B 276 (1991) 249; Phys. Rev. Lett. 68 (1992) 9.
- [56] G.R. Smith, A.D. Bruce, J. Phys. A 28 (1995) 6623.
- [57] G.M. Torrie, J.-P. Valleau, J. Comput. Phys. 23 (1997) 187.
- [58] R.H. Swendsen, J.-S. Wang, Phys. Rev. Lett. 57 (1986) 2607.

- [59] C.J. Geyer, in *Computing Science and Statistics: Proceedings of the 23rd Symposium on the interface*, ed. E.K. Keramidas, Interface Foundation, Fairfax Station, New York, 1991, p. 156.
- [60] E. Marinari, G. Parisi, *Europhys. Lett.* 19 (1992) 451.
- [61] A.P. Lyubartsev, A.A. Martsinovskii, S.V. Shevkunov, P.N. Vorontsov-Velyaminov, *J. Chem. Phys.* 96 (1992) 1776.
- [62] K. Hukushima, K. Nemoto, *J. Phys. Soc. Jpn.* 65 (1996) 1604.
- [63] E. Marinari, G. Parisi, J. Ruiz-Lorenzo, in *Spin Glasses and Random Fields*, ed. A.P. Young, *Directions in Condensed Matter Physics*, World Scientific, Singapore, 1998, Vol. 12.
- [64] C. Yamaguchi, Y. Okabe, *J. Phys. A* 34 (2001) 8781; P.N. Vorontsov-Velyaminov, N.A. Volkov, A.A. Yurchenko, *J. Phys. A* 37 (2004) 1573; N. Rathore, J.J. de Pablo, *J. Chem. Phys.* 116 (2002) 7225; M.S. Shell, P.G. Debenedetti, A.Z. Panagiotopoulos, *Phys. Rev. E* 66 (2003) 056703; P. Poulain, F. Calvo, R. Antoine, M. Broyer, Ph. Dugourd, *ibid.* 73 (2006) 056704; C. Zhou, T.C. Schulthess, S. Torbrügge, D.P. Landau, *Phys. Rev. Lett.* 96 (2006) 120201.
- [65] B.J. Schulz, K. Binder, M. Muller, *Int. J. Mod. Phys. C* 13 (2002) 477.
- [66] A. Malakis, S.S. Martinos, I.A. Hadjiagapiou, A.S. Peratzakis, *Int. J. Mod. Phys. C* 15 (2004) 729.
- [67] P. Dayal, S. Trebst, S. Wessel, D. Würtz, M. Troyer, S. Sabhapandit, S.N. Coppersmith, *Phys. Rev. Lett.* 92 (2004) 097201.
- [68] C. Zhou, R.N. Bhatt, *Phys. Rev. E* 72 (2005) 025701(R).
- [69] N. Schreider, J. Adler, *J. Phys. A* 38 (2005) 7253.
- [70] H. Behringer, M. Pleimling, *Phys. Rev. E* 74 (2006) 011108.
- [71] M. Pleimling, A. Hüller, *J. Stat. Phys.* 104 (2001) 971.
- [72] K. Binder, *Physica A* 319 (2003) 99.
- [73] S.S. Martinos, A. Malakis, I.A. Hadjiagapiou, *Physica A* 366 (2006) 273.
- [74] D. Ledue, D.P. Landau, J. Teillet, *J. Appl. Phys.* 83 (1998) 6305.
- [75] K. Binder, *Z. Phys. B* 43 (1981) 119.
- [76] H.W.J. Blöte, M.P. Nightingale, *Physica A* 112 (1982) 405.
- [77] V. Privman, M.E. Fisher, *J. Stat. Phys.* 33 (1983) 385.
- [78] C. Borgs, R. Kotecký, *J. Stat. Phys.* 61 (1990) 79; *Phys. Rev. Lett.* 68 (1992) 1734; *Physica A* 194 (1993) 128.
- [79] C. Borgs, R. Kotecký, S. Miracle-Solé, *J. Stat. Phys.* 62 (1991) 529.
- [80] C. Borgs, S. Kappler, *Phys. Lett. A* 171 (1992) 37.

- [81] C. Borgs, J.Z. Imbrie, *Commun. Math. Phys.* 145 (1992) 235.
- [82] C. Borgs, *Nucl. Phys. B* 384 (1992) 605.
- [83] S. Pirogov, Ya.G. Sinai, *Theor. Math. Phys. Engl. Transl.* 25 (1975) 1185; 26 (1976) 39.
- [84] M. Zahradník, *Commun. Math. Phys.* 93 (1984) 559.
- [85] C. Borgs, J.Z. Imbrie, *Commun. Math. Phys.* 123 (1989) 305.
- [86] P.A. Slotte, P.C. Hemmer, *J. Phys. C* 17 (1984) 4645.
- [87] R.J. Baxter, *J. Phys. C* 6 (1973) L445.
- [88] T. Kihara, Y. Midzuno, T. Shizume, *J. Phys. Soc. Jpn.* 9 (1954) 681.

Table 1

Exact results for the bulk energies e_o and e_d , the latent heat Δe [87,88], and the values of $V_4(\infty)|_{min}$ and $U_2(\infty)|_{max}$ [16,27] for the $q = 10$, $q = 8$, $q = 6$, and $q = 5$ Potts model in two dimensions. The last row refers to the $R = 1$ triangular SAF model.

Model	e_o	e_d	Δe	$V_4(\infty) _{min}$	$U_2(\infty) _{max}$
$q = 10$ Potts	-1.66425	-0.96820	0.696	0.5589	1.0751
$q = 8$ Potts	-1.59673	-1.11037	0.486	0.6207	1.0333
$q = 6$ Potts	-1.50875	-1.30775	0.201	0.6598	1.0051
$q = 5$ Potts	-1.47367	-1.42075	0.053	0.6662	1.0003
Tr. SAF	-1.61784(728)	-1.48852(565)	0.129(12)	0.66435(33)	1.00174(25)

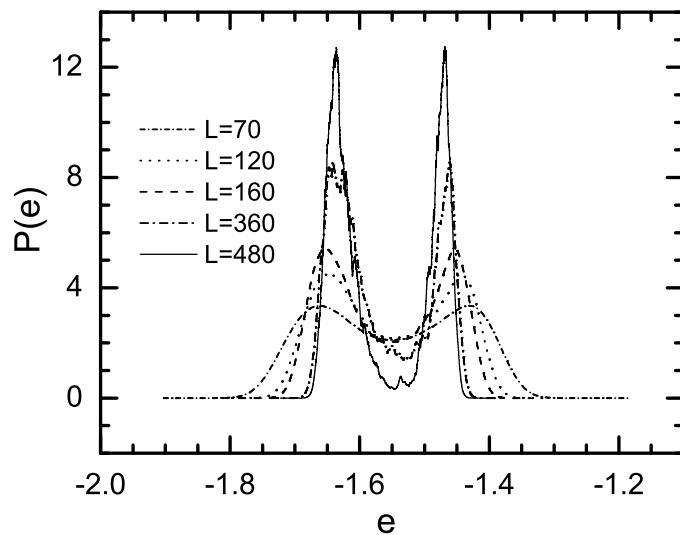


Fig. 1. Energy distributions at T_h for the $R = 1$ triangular SAF model for selected lattice sizes.

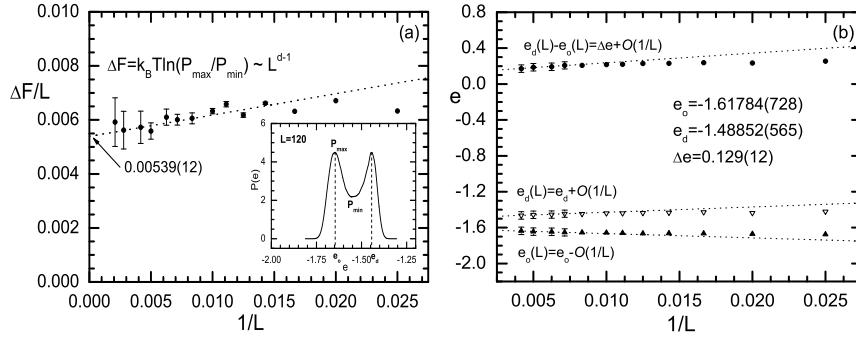


Fig. 2. (a) Plot of the barrier height $\Delta F(L)L^{-d+1}$. The dotted line is an extrapolation to $L \rightarrow \infty$, giving a nonzero value for the surface tension of the order of 0.00539(12). The inset is used as a guide for the reader. (b) The energy minima $e_o(L)$ and $e_d(L)$ and their difference as a function of the inverse linear size. The dotted lines are linear fits indicating the values of the bulk energies e_o and e_d , and that of the latent heat Δe at $L = \infty$.

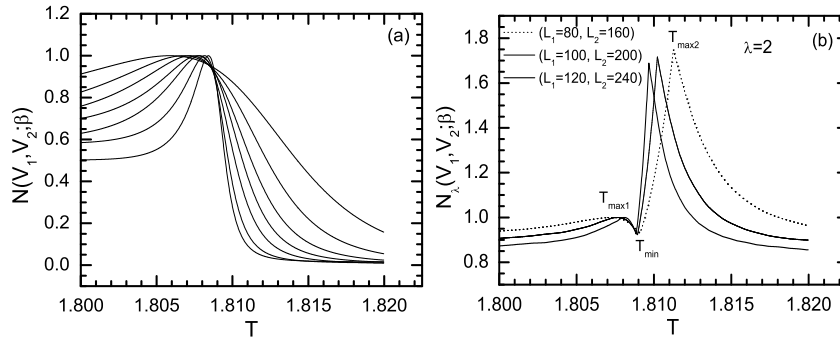


Fig. 3. Temperature-dependence of the ratios $N(V_1, V_2; \beta)$ (a) and $\tilde{N}_{\lambda=2}(V_1, V_2; \beta)$ (b) (Eqs. (24) and (30), respectively). In panel (a) all pairs are shown, i.e. $(L_1, L_2) = (40, 80), (50, 100), (60, 120), (70, 140), (80, 160), (100, 200),$ and $(120, 240)$, while in panel (b) only the pairs $(L_1, L_2) = (80, 160), (100, 200),$ and $(120, 240)$ are shown.

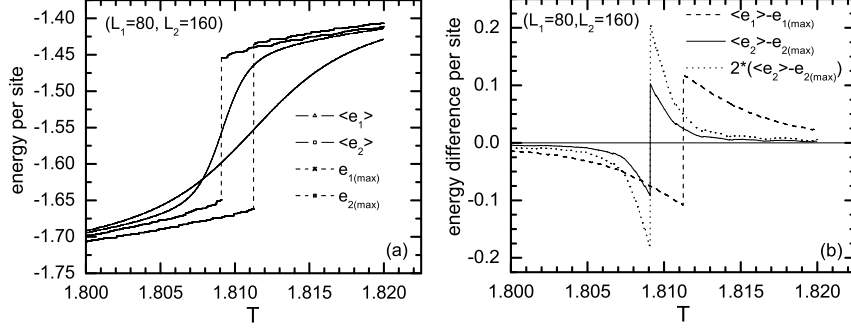


Fig. 4. (a) Illustration of the crossing point corresponding to the peak of the number-of-phases parameter. The behavior of the most probable energies of the pair of systems is also illustrated. (b) Behavior of the differences, $\langle e \rangle - \tilde{e}$, of the two characteristic energies for each system of the chosen pair. For the larger lattice the graph corresponding to the double of the difference $\langle e \rangle - \tilde{e}$ is also shown in order to facilitate the illustration of the crossing relationship (31) for $\lambda = 2$ ($\alpha = 4$).

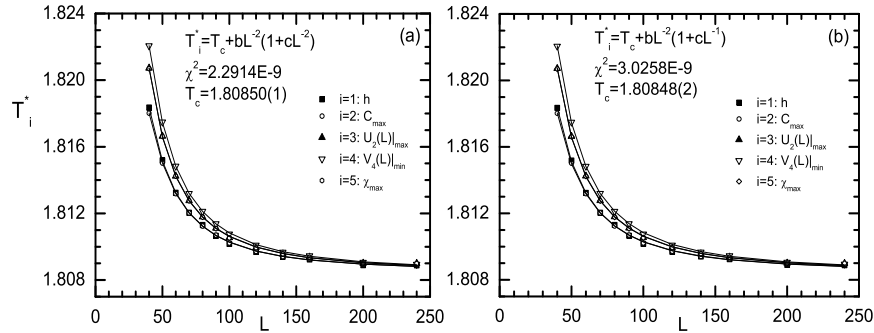


Fig. 5. (a) Simultaneous fittings for the shifting of all pseudocritical temperatures T_i^* using an L^{-2} correction. (b) The same with panel (a) but with an L^{-1} correction.

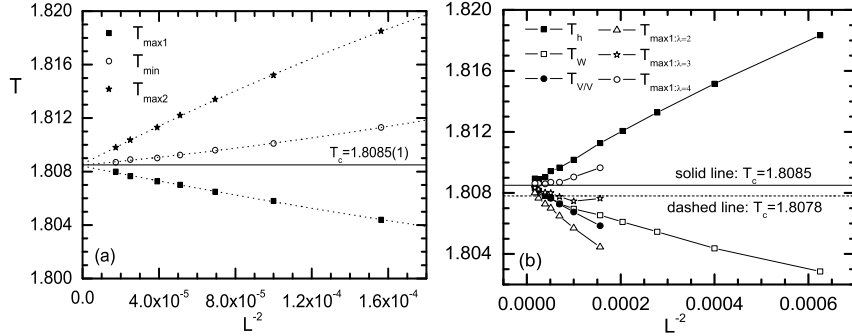


Fig. 6. (a) Illustration of the behavior of the three peaks of the reduced number-of-phases parameter defined in in Eq. (30) for $\lambda = 2$. (b) Behavior of six finite-size transition points and comparison with our estimate (solid line) for the transition point and also with the estimate $T_c = 1.8078$ of Ref. [14] (dashed line).

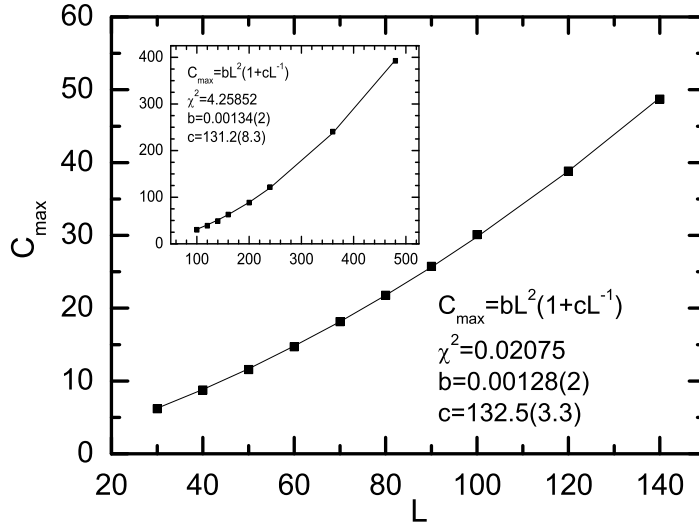


Fig. 7. FSS behavior of the specific heat peaks in two lattice ranges: $L = 30 - 140$ and $L = 100 - 480$ (inset). An L^{-1} correction has been added to the L^2 divergence.

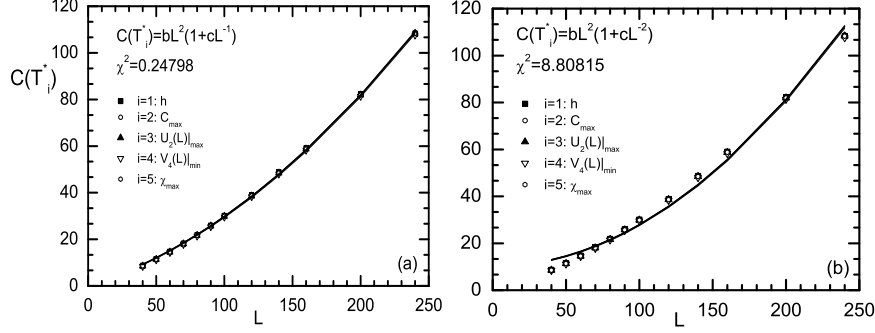


Fig. 8. (a) FSS behavior of the specific heat data at the five pseudocritical temperatures T_i^* using an L^{-1} correction. (b) The same with panel (a) but with an L^{-2} correction. Note the large difference in the χ^2 values.

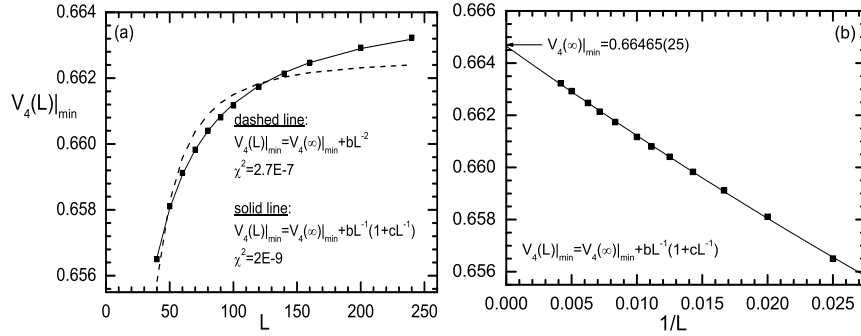


Fig. 9. (a) FSS behavior of $V_4(L)|_{min}$. Two fitting attempts are applied as shown in the figure. χ^2 is much smaller for the case of an L^{-1} correction. (b) FSS of $V_4(L)|_{min}$, now against L^{-1} . The line corresponds to the fitting formulae shown in panel (b) and gives an estimate $V_4(\infty)|_{min} = 0.66465(25)$.

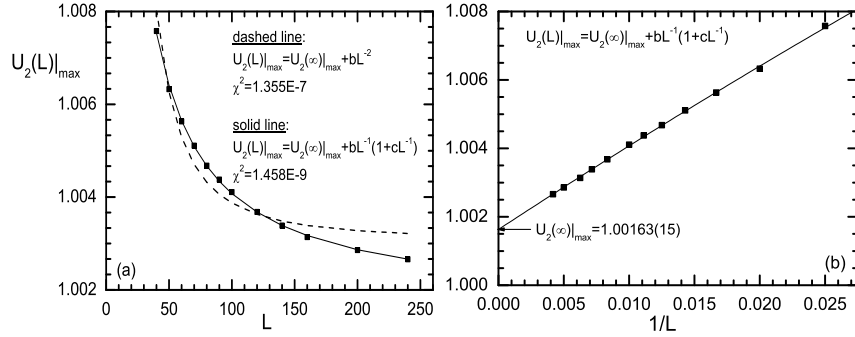


Fig. 10. (a) The same as in Fig. 9 for $U_2(L)|_{max}$. (b) FSS of $U_2(L)|_{max}$, against L^{-1} . The solid line corresponds to the fitting formulae shown in panel (b) and produces the estimate $U_2(\infty)|_{max} = 1.00163(15)$.

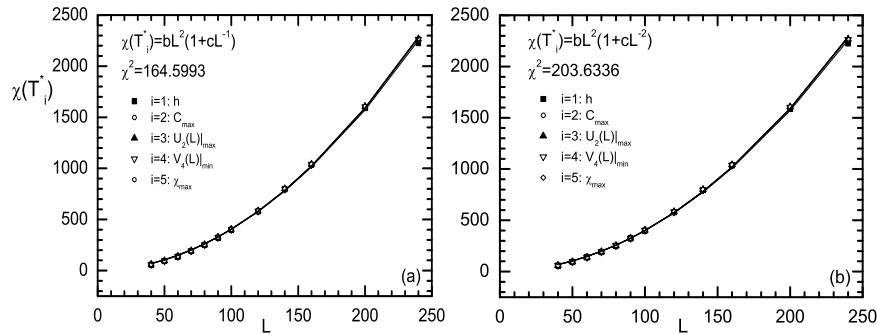


Fig. 11. (a) FSS behavior of the susceptibility data at the five pseudocritical temperatures T_i^* . The solid lines are simultaneous fitting attempts, using an L^{-1} correction. (b) The same with panel (a) but with a correction of the order of L^{-2} .